

On the Performance of the Extended EWMA Control Chart for Monitoring Process Mean Based on Autocorrelated Data

Kotchaporn Karoon, Yupaporn Areepong* and Saowanit Sukparungsee

Department of Applied Statistics, Faculty of Applied Science, King Mongkut's University of Technology North Bangkok, Bangkok, Thailand

* Corresponding author. E-mail: yupaporn.a@sci.kmutnb.ac.th DOI: 10.14416/j.asep.2023.01.004

Received: 4 October 2022; Revised: 26 October 2022; Accepted: 6 December 2022; Published online: 13 January 2023

© 2023 King Mongkut's University of Technology North Bangkok. All Rights Reserved.

Abstract

The extended exponentially weighted moving average (EEWMA) control chart is an instrument for detection. It can quickly identify small shifts in the process. The benchmark for the control chart's performance is the average run length (*ARL*). In this paper, we present the efficiency of the EEWMA control chart to detect tiny shifts when the observations are autocorrelated with exponential residuals through the explicit formulas of the *ARL*. The accuracy of the solution was verified with the numerical integral equation (NIE) method. After that, the *ARL* effectiveness of the *ARL* on the EEWMA control chart was expanded to compare with the traditional EWMA control chart. Finally, using two real datasets that indicate the percentages of internet users using Windows 7 and iOS, the applicability of the offered method is shown. Our findings support the notion that the EEWMA control chart performs better when using autocorrelated data to track tiny changes.

Keywords: Average run length, Autoregressive process, EEWMA control chart, EWMA control chart, Explicit formulas

1 Introduction

One of the instruments for statistical process control (SPC) is control charts. It has numerous applications and is frequently used in the manufacturing sector to monitor, regulate and improve processes [1], [2]. The Shewhart chart is a common name for the standard control chart [3], which is more efficient at detecting large shifts in the monitored mean process. Standard process monitoring techniques, such as the exponentially weighted moving average (EWMA) chart, and the cumulative sum (CUSUM) chart, have undergone several changes and expansions. The EWMA control chart [4] and the CUSUM control chart [5] are developed to detect small shifts in the process. Next, the modified EWMA control chart was suggested by Patel and Divecha [6] and developed by Khan *et al.* [7]. For the autocorrelation observations, it performs well at quickly detecting slight size shifts. Later, Naveed *et al.* [8] presented the extended exponentially

weighted moving average (EEWMA) control chart. It can detect slight shifts in the process more quickly.

One of the comparative performance methods for control charts, the average run length (*ARL*), can be classified into two categories: The expected number of observations of an in-control process, or ARL_0 , that should be made before an out-of-control observation is discovered. ARL_0 should be large. Meanwhile, ARL_1 refers to the expected number of observations gathered from out-of-control and the smallest size is ideal. Many previous studies have focused on approximating the *ARL* to evaluate an efficient control chart using many methods. For example, Mastrangelo and Montgomery [9] used the classic EWMA chart with the Monte Carlo simulation approach to display the *ARL* for serially correlated observations. Chananet *et al.* [10] used a Markov chain method to generate the CUSUM and EWMA charts under the zero-inflated negative binomial model. Sukparungsee [11] used the Martingale technique to approximate the *ARL*. Karoon

et al. [12] used the NIE technique to approximate the *ARL* on the EEWMA control chart. It was compared to the performance of the other methods.

In addition, many researchers have used explicit formulas to evaluate the *ARL* values of the control charts. Suriyakat *et al.* [13] solved the explicit formulas of the *ARL* on the exponential AR(1) with the trend process in the EWMA control chart. Petcharat *et al.* [14] proposed the explicit formulas for the *ARL* on the EWMA control chart under the observations of the MA(q) model. When using seasonal AR(p) models for the data, Busababodin [15] provided an explicit technique for calculating the *ARL* on the CUSUM control chart. Paichit [16] presented an analytical solution for the *ARL* on the CUSUM control chart for first-order data with explanatory variables in the ARX(1) model. Phanyaem [17] developed the *ARL* on CUSUM chart analytical formula for the seasonal ARMA(1,1) model. Sukparungsee and Areepong [18] developed the explicit formulas for the *ARL* on the EWMA chart based on the AR(p) process. Afterward, Areepong [19] proposed the explicit formulas on the MA chart under, which the observations are binomially distributed. The Modified-mxEWMA chart developed by Anwar *et al.* [20] shows how the wood industry has used the method and can identify small-to-medium shifts in the monitoring process. Sunthornwat and Areepong [21] derive the explicit formulas for the *ARL* of the CUSUM chart under seasonal and non-seasonal moving average models with the observations of the exogenous variables. Saghir *et al.* [22] suggested a modified EWMA chart, and the *ARL* evaluated its effectiveness. Recently, Phanthuna *et al.* [23] presented the explicit formulas for calculating the *ARL* of the two-sided modified EWMA control chart for the first-order autoregressive process. Moreover, the explicit formula for the *ARL* is solved by the modified EWMA control chart for the stationary AR(1) with trend observation, which was developed by Phanthuna [24] in the same year. Moreover, Karoon *et al.* [25] presented the *ARL* that is designed by explicit formulas when the observations are the AR(p) process with white noise residuals.

However, no prior research has been done on the precise formulations of the *ARL* for the quadratic trend AR(p) model on the extended EWMA chart. In addition, the goal of this research is to derive the explicit formulas for the *ARL* on the extended EWMA chart based on

quadratic trend autoregressive models—specifically, quadratic trend AR(1) and quadratic trend AR(2) models with exponential white noise. These were expanded to compare with various and the EWMA control chart. Furthermore, for both simulated and real-world datasets, the explicit formula efficacy for computing the *ARL* on the extended EWMA control chart was compared to the standard EWMA control chart with both simulated data and real-world dataset.

2 Materials and Methods

2.1 Exponentially Weighted Moving Average control chart (EWMA)

The EWMA chart was proposed by Robert [4]. It is frequently used to find small adjustments in the monitoring process. The EWMA statistic may be expressed using the following in Equation (1):

$$Z_t = (1 - \lambda)Z_{t-1} + \lambda X_t, \quad t = 1, 2, \dots \quad (1)$$

where X_t is an observation, which is a sequence of quadratic trend model, λ is a parameter of exponential smoothing with $\lambda \in (0, 1]$, Z_0 is the initial value of the EWMA statistic, $Z_0 = u$.

The upper and lower control limits (*UCL* and *LCL*) shown in Equation (2) are

$$UCL = \mu + Q_z \sigma \sqrt{\frac{\lambda}{2 - \lambda}} \quad \text{and} \quad LCL = \mu - Q_z \sigma \sqrt{\frac{\lambda}{2 - \lambda}} \quad (2)$$

where Q_z is a control limit width, μ is a mean in the process and σ is a standard deviation in the process. The stopping time is determined by $\tau_z = \inf\{t \geq 0 : Z_t < a, Z_t > h\}$ and then h is *UCL* and *LCL* is .

2.2 Extended Exponentially Weighted Moving Average control chart (EEWMA)

Naveed *et al.* [8] presented the EEWMA chart. It is a modification of the traditional EWMA chart. The performance control chart is very good at seeing even the smallest changes in the monitored process. The following equation in Equation (3) can be used to

express the EEWMA statistic.

$$E_t = \lambda_1 X_t - \lambda_2 X_{t-1} + (1 - \lambda_1 + \lambda_2) E_{t-1}, \quad t = 1, 2, \dots \quad (3)$$

where X_t is an observation, which is a sequence of quadratic trend model, λ_1 and λ_2 are exponential smoothing parameters with $\lambda_1 \in (0, 1)$ and $\lambda_2 \in (0, \lambda_1)$, E_0 is the initial value of the EEWMA statistic, $E_0 = u$.

The upper and lower control limits (UCL and LCL) shown in Equation (4) are

$$UCL = \mu_0 + Q_E \sigma \sqrt{\frac{\lambda_1^2 + \lambda_2^2 - 2\lambda_1\lambda_2(1 - \lambda_1 + \lambda_2)}{2(\lambda_1 - \lambda_2) - (\lambda_1 - \lambda_2)^2}} \quad \text{and}$$

$$LCL = \mu_0 - Q_E \sigma \sqrt{\frac{\lambda_1^2 + \lambda_2^2 - 2\lambda_1\lambda_2(1 - \lambda_1 + \lambda_2)}{2(\lambda_1 - \lambda_2) - (\lambda_1 - \lambda_2)^2}} \quad (4)$$

where Q_E is a control limit width, μ is a mean in the process and σ is a standard deviation in the process. The stopping time is determined by $\tau_E = \inf\{t \geq 0 : E_t < a, E_t > b\}$ and then b is UCL and a is LCL.

2.3 The explicit formula of the ARL on the EEWMA control chart for quadratic trend AR(p) model

For a random variable sequence, X_t is an observation of a quadratic trend AR(p) model. The quadratic trend AR(p) model can be expressed in Equation (5) as follows:

$$X_t = \eta + \beta t + \gamma t^2 + \phi_1 X_{t-1} + \phi_2 X_{t-2} + \dots + \phi_p X_{t-p} + \varepsilon_t \quad (5)$$

where η, β, γ are constants of the quadratic trend model, ϕ_i is an autoregressive coefficient at $i = 1, 2, \dots, p$ or ($|\phi_p| < 1$). ε_t is a white noise with exponential distribution. ($\varepsilon_t \sim \text{Exp}(\alpha)$). The EEWMA statistic E_t is given as follows

$$E_t = \lambda_1 (\eta + \beta + \gamma + \sum_{i=1}^p \phi_i X_{t-i} + \varepsilon_t) - \lambda_2 X_{t-1} + (1 - \lambda_1 + \lambda_2) E_0.$$

And then, it can be rearranged in Equation (6) as follows:

$$E_t = \lambda_1 \eta + \lambda_1 \beta + \lambda_1 \gamma + (1 - \lambda_1 + \lambda_2) E_0 + (\lambda_1 \phi_1 - \lambda_2) X_{t-1} + \lambda_1 \sum_{i=2}^p \phi_i X_{t-i} + \lambda_1 \varepsilon_t. \quad (6)$$

where E_t is in an in-control process can be reorganized in the error term ε_1 as:

$$\frac{a - (1 - \lambda_1 + \lambda_2)u - (\lambda_1 \phi_1 - \lambda_2) X_{t-1}}{\lambda_1} - \sum_{i=2}^p \phi_i X_{t-i} - \eta - \beta - \gamma < \varepsilon_1$$

$$< \frac{b - (1 - \lambda_1 + \lambda_2)u - (\lambda_1 \phi_1 - \lambda_2) X_{t-1}}{\lambda_1} - \sum_{i=2}^p \phi_i X_{t-i} - \eta - \beta - \gamma$$

Let $C(u)$ denotes the ARL on the EEWMA chart for the quadratic trend AR(p) observations. The function $C(u)$, as shown in Equation (7), can be calculated using the Fredholm integral equation of the second type [26], which is presented as follows:

$$C(u) = 1 + \int C(E_1) f(\varepsilon_1) d\varepsilon_1 \quad (7)$$

Consequently, the following is how the function $C(u)$ is expressed in Equation (8):

$$C(u) = 1 + \int_{\frac{a - (1 - \lambda_1 + \lambda_2)u - (\lambda_1 \phi_1 - \lambda_2) X_{t-1}}{\lambda_1} - \sum_{i=2}^p \phi_i X_{t-i} - \eta - \beta - \gamma}^{\frac{b - (1 - \lambda_1 + \lambda_2)u - (\lambda_1 \phi_1 - \lambda_2) X_{t-1}}{\lambda_1} - \sum_{i=2}^p \phi_i X_{t-i} - \eta - \beta - \gamma} L \left(\begin{array}{l} \lambda_1 \eta + \lambda_1 \beta + \lambda_1 \gamma \\ + (1 - \lambda_1 + \lambda_2)u \\ + (\lambda_1 \phi_1 - \lambda_2) X_{t-1} \\ + \lambda_1 \sum_{i=2}^p \phi_i X_{t-i} \\ + \lambda_1 \gamma \end{array} \right) f(y) dy. \quad (8)$$

When

$$k = \lambda_1 \eta + \lambda_1 \beta + \lambda_1 \gamma + (1 - \lambda_1 + \lambda_2)u + (\lambda_1 \phi_1 - \lambda_2) X_{t-1} + \lambda_1 \sum_{i=2}^p \phi_i X_{t-i} + \lambda_1 \varepsilon_1$$

is specified in order to modify the integration variable, $C(u)$ is rearranged as:

$$C(u) = 1 + \frac{1}{\lambda_1} \int_a^b C(k) f \left(\frac{k - (1 - \lambda_1 + \lambda_2)u - (\lambda_1 \phi_1 - \lambda_2) X_{t-1}}{\lambda_1} - \sum_{i=2}^p \phi_i X_{t-i} - \eta - \beta - \gamma \right) dk. \quad (9)$$

If $\varepsilon_t \sim \text{Exp}(\alpha)$ then $C(u)$ is shown in Equation (10) as:

$$C(u) = 1 + \frac{1}{\lambda_1 \alpha} e^{\frac{(1 - \lambda_1 + \lambda_2)u + (\lambda_1 \phi_1 - \lambda_2) X_{t-1} + \sum_{i=2}^p \phi_i X_{t-i} + \eta + \beta + \gamma}{\lambda_1 \alpha}} \int_a^b C(k) e^{-\frac{k}{\lambda_1 \alpha}} dk \quad (10)$$

where



$$D(u) = e^{\frac{(1-\lambda_1+\lambda_2)u+(\lambda_1\phi_1-\lambda_2)X_{t-1} + \sum_{i=2}^p \phi_i X_{t-i} + \eta + \beta + \gamma}{\lambda_1 \alpha}},$$

$$L = \int_a^b C(k) e^{-\frac{k}{\lambda_1 \alpha}} dk.$$

Consequently, $C(u) = 1 + \frac{D(u)}{\lambda_1 \alpha} L.$ (11)

Next, substitute Equation (11) into the constant L to solve for the constant L ,

$$L = \frac{-\lambda_1 \alpha (e^{-\frac{b}{\lambda_1 \alpha}} - e^{-\frac{a}{\lambda_1 \alpha}})}{\frac{(\lambda_1 \phi_1 - \lambda_2) X_{t-1}}{\lambda_1 \alpha} + 1 + \frac{1}{\lambda_1 - \lambda_2} \cdot e^{\frac{\sum_{i=2}^p \phi_i X_{t-i} + \eta + \beta + \gamma}{\alpha}} \cdot (e^{-\frac{(\lambda_1 - \lambda_2)b}{\lambda_1 \alpha}} - e^{-\frac{(\lambda_1 - \lambda_2)a}{\lambda_1 \alpha}})}$$
 (12)

Substituting constant $C(u)$ from Equation (12) with Equation (11), then can be assigned as

$$C(u) = 1 - \frac{(\lambda_1 - \lambda_2) e^{\frac{(1-\lambda_1+\lambda_2)u}{\lambda_1 \alpha}} \cdot (e^{-\frac{b}{\lambda_1 \alpha}} - e^{-\frac{a}{\lambda_1 \alpha}})}{(\lambda_1 - \lambda_2) e^{\left[\frac{(\lambda_1 \phi_1 - \lambda_2) X_{t-1}}{\lambda_1 \alpha} + \frac{\sum_{i=2}^p \phi_i X_{t-i} + \eta + \beta + \gamma}{\alpha} \right]} + (e^{-\frac{(\lambda_1 - \lambda_2)b}{\lambda_1 \alpha}} - e^{-\frac{(\lambda_1 - \lambda_2)a}{\lambda_1 \alpha}})}$$
 (13)

Therefore, the solution of Equation (13) is an explicit formula of ARL on the $EEWMA$ control chart for the quadratic trend $AR(p)$ model. The in-control process is $\alpha = \alpha_0$, whereas the out-of-control process is $\alpha = \alpha_1$ as well as $\alpha_1 = (1 + \delta)\alpha_0$, and δ is the shift size in the process.

2.4 Numerical integral equation of the ARL on the $EEWMA$ control chart for the quadratic trend $AR(p)$ models

Equation (9) is used to generate the numerical integral equation (NIE) technique for accuracy with the ARL of the explicit formula. Let $\tilde{C}(u)$ be the estimated ARL value that is used by the composite midpoint quadrature rule [12]. It is approximated by Gauss-Legendre’s rule

that can be represented by Equation (14).

$$\int_a^b C(k) f(k) dk \approx \sum_{j=1}^m w_j f(a_j)$$
 (14)

The m linear equation system is presented as follows:

$$C_{m \times 1} = 1_{m \times 1} + R_{m \times m} C_{m \times 1} \text{ or}$$

$$(I_m - R_{m \times m}) C_{m \times 1} = 1_{m \times 1} \text{ or}$$

$$C_{m \times 1} = (I_m - R_{m \times m})^{-1} 1_{m \times 1}$$

where $C_{m \times 1} = [\tilde{C}(a_1), \tilde{C}(a_2), \tilde{C}(a_3), \dots, \tilde{C}(a_m)]^T$, $1_{m \times 1} = [1, 1, \dots, 1]^T$ and $I_m = \text{diag}(1, 1, \dots, 1)$.

Let $I_{m \times m}$ be a matrix. The m to m^{th} element of R is defined as the solution to the m linear equation, which is shown as follows:

$$[R_{ij}] \approx \frac{1}{\lambda_1} w_j f \left(\frac{s_j - (1 - \lambda_1 + \lambda_2)s_j - (\lambda_1 \phi_1 - \lambda_2)X_{t-1} - \phi_2 X_{t-2} - \dots - \phi_p X_{t-p} - \eta - \beta - \gamma}{\lambda_1} \right)$$

Lastly, the solution of Equation (15) is a numerical estimate for the function $\tilde{C}(u)$:

$$\tilde{C}(u) = 1 + \frac{1}{\lambda_1} \sum_{j=1}^m w_j C(s_j) f \left(\frac{s_j - (1 - \lambda_1 + \lambda_2)u - (\lambda_1 \phi_1 - \lambda_2)X_{t-1} - \phi_2 X_{t-2} - \dots - \phi_p X_{t-p} - \eta - \beta - \gamma}{\lambda_1} \right)$$
 (15)

when s_j is a group of the division point on the interval $[a, b]$ as $s_j = (j-0.0)w_j + a$, $j = 1, 2, 3, \dots, m$ and then w_j is a weight of the composite midpoint formula $w_j = \frac{b-a}{m}$.

2.5 The ARL ’s existence and uniqueness

Let T represent a continuous function that operates under the categories of all.

$$T(C(u)) =$$

$$1 + \frac{1}{\lambda_1} \int_a^b C(k) f \left(\frac{k - (1 - \lambda_1 + \lambda_2)u - (\lambda_1 \phi_1 - \lambda_2)X_{t-1} - \sum_{i=2}^p \phi_i X_{t-i} - \eta - \beta - \gamma}{\lambda_1} \right) dk$$
 (16)

The fixed-point equation $T(C(u)) = C(u)$ has a unique solution if operator T is a contraction.

Theorem 1 Banach’s Fixed-point Theorem:

Let $T = X \rightarrow X$ represent a mapping of contractions with the contraction constant $r \in [0,1)$, and let X represent a whole metric space.

There is a unique $C(\cdot) \in X$, and then $T(C(u)) = C(u)$, i.e., a unique fixed-point in X . Next step, C_1, C_2 are given to be a solution to Equation (9) for all $C_1, C_2 \in X$, such that $\|T(C_1) - T(C_2)\| \leq r \|C_1 - C_2\|$ is proved as follows below.

Proof: Let T be a contraction mapping as specified in Equation (16) for all $C_1, C_2 \in u[a,b]$,

Thus, $\|T(C_1) - T(C_2)\| \leq r \|C_1 - C_2\|, \forall C_1, C_2 \in u[a,b]$ with $r \in [0,1)$ under the norm $\|C\|_\infty = \sup_{u \in [a,b]} |C(u)|$, so $\|T(C_1) - T(C_2)\|_\infty$

$$\begin{aligned} &= \sup_{u \in [a,b]} \left| \frac{1}{\lambda_1 \alpha} e^{\frac{(1-\lambda_1+\lambda_2)u+(\lambda_1\phi_1-\lambda_2)X_{i-1} + \sum_{j=2}^i \phi_j X_{i-j} + \eta + \beta + \gamma}{\lambda_1 \alpha}}}{\int_a^b (C_1(k) - C_2(k)) e^{-\frac{b}{\lambda_1 \alpha} k} dk} \right| \\ &\leq \sup_{u \in [a,b]} \left| C_1 - C_2 \right| \frac{1}{\lambda_1 \alpha} e^{\frac{(1-\lambda_1+\lambda_2)u+(\lambda_1\phi_1-\lambda_2)X_{i-1} + \sum_{j=2}^i \phi_j X_{i-j} + \eta + \beta + \gamma}{\lambda_1 \alpha}} \cdot \left(-\lambda_1 \alpha \right) \left(e^{-\frac{b}{\lambda_1 \alpha}} - e^{-\frac{a}{\lambda_1 \alpha}} \right) \\ &= \|C_1 - C_2\|_\infty \sup_{u \in [a,b]} \left| e^{\frac{(1-\lambda_1+\lambda_2)u+(\lambda_1\phi_1-\lambda_2)X_{i-1} + \sum_{j=2}^i \phi_j X_{i-j} + \eta + \beta + \gamma}{\lambda_1 \alpha}} \right| \cdot \left| e^{-\frac{a}{\lambda_1 \alpha}} - e^{-\frac{b}{\lambda_1 \alpha}} \right| \\ &\leq r \|C_1 - C_2\|_\infty. \end{aligned}$$

3 Results

To compare the ARL solution of the explicit formulas and NIE method for the ARL results, the absolute relative change (ARC) [27] is computed as follows:

$$ARC(\%) = \frac{|C(u) - \tilde{C}(u)|}{C(u)} \times 100 \tag{17}$$

Moreover, the relative mean index (RMI) [28] is employed to evaluate each control chart's effectiveness under different λ conditions. The RMI is calculated using the formula shown below:

$$RMI = \frac{1}{n} \sum_{i=1}^n \left[\frac{ARL_i(c) - ARL_i(s)}{ARL_i(s)} \right] \tag{18}$$

where $ARL_i(c)$ is ARL of each control chart for the determined shift sizes of row i , $ARL_i(s)$ is the lowest ARL of row from all control charts. The control chart had the best performance in change detection, as seen by the control chart's lowest RMI score.

3.1 Experimental results

For this section, a simulation of the in-control process is typically given $ARL_0 = 370$ and then the initial parameter value was studied at $\alpha_0 = 1$. The out-of-control process, $\alpha_1 = (1 + \delta)\alpha_0$ is computed by determining shift sizes (δ) to be 0.001, 0.002, 0.003, 0.005, 0.01, 0.03, 0.05, 0.1, 0.5 and 1. Since the lower bound α is studied on the exponential distribution of ε_i , which is in the interval $[0, \infty)$, the upper bound b is found by using the least a to be 0. Additionally, the CPU time (PC System: windows10, 64-bit, Intel® Core™ i5-8250U 1.60 GHz 1.80 GHz, RAM 4 GB) was also supplied to compute the speed test results in seconds. MATHEMATICA® was used to compute the analytical outcomes.

In Tables 1 and 2, the ARL of the EEWMA control chart at $\lambda_2 = 0.01$ is computed by using two techniques such that the explicit formula and NIE method with various λ_1 and ϕ_i for the quadratic trend AR(1) and quadratic trend AR(2) models. The findings show that the ARL values produced using explicit formulas provide outcomes that are comparable to those of NIE. The computational time durations for the analytical solutions are about 3 s whereas the computational time for the explicit formula is almost instantaneous. Both solutions have the ARC%, which is calculated from Equation (17), the value was shown as less than 0.00023%.

The efficiency of control charts is shown by the quadratic trend AR(1) model in Table 3 and Figure 1 and the quadratic trend AR(2) model in Table 4 and Figure 3. The finding indicates that the EEWMA control chart can be effectively detected to be faster than the EWMA control chart for minor changes. Correspondingly, the RMI , which is computed from Equation (18), the results were shown that the RMI of the EEWMA control charts various λ_2 is lower than the EWMA control chart. In addition, the EEWMA control chart has higher efficiency if λ_2 is increased.

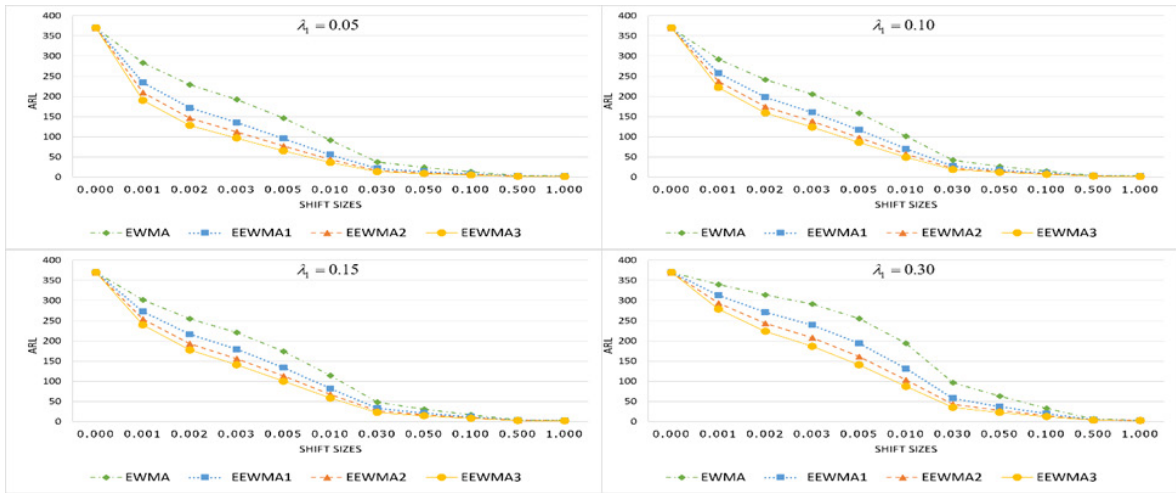


Figure 1: ARL comparing of the EWMA and the EEWMA with different λ_1 control charts for the quadratic trend AR(1) model based on various λ_1 situations

Table 1: Comparing the ARL_0 from two techniques for the quadratic trend AR(1) model on the EEWMA control chart at $\lambda_1 = 0.05, \lambda_2 = 0.01, \eta = 0.01, \beta = 0.1$ and $\gamma = 0.1$

ϕ_1	b	Explicit Formula (Computational Time)	NIE Method (Computational Time)	ARC%
0.1	0.03063686	370.0392251 (<0.1)	370.0391840 (2.970)	0.000011
0.2	0.04154282	370.0530132 (<0.1)	370.0529344 (2.578)	0.000021
0.3	0.05642129	370.0174970 (<0.1)	370.0173433 (2.531)	0.000042
-0.1	0.01671633	370.0470954 (<0.1)	370.0470837 (3.001)	0.000003
-0.2	0.01236109	370.0417634 (<0.1)	370.0417572 (2.533)	0.000002
-0.3	0.00914490	370.0354831 (<0.1)	370.0354797 (2.624)	0.000001

Table 2: Comparing the ARL_0 from two techniques for the quadratic trend AR(2) model on the EEWMA control chart at $\lambda_1 = 0.05, \lambda_2 = 0.01, \eta = 0.01, \beta = 0.1$ and $\gamma = 0.1$

ϕ_1	ϕ_2	b	Explicit Formula (Computational Time)	NIE Method (Computational Time)	ARC%
0.1	0.1	0.02262059	370.0331986 (<0.1)	370.0331769 (3.046)	0.000006
	-0.1	0.03390498	370.0633411 (<0.1)	370.0632902 (3.093)	0.000014
0.2	0.2	0.02768736	370.0641122 (<0.1)	370.0640790 (2.733)	0.000009
	-0.2	0.06251077	370.0537848 (<0.1)	370.0535916 (2.594)	0.000052
0.3	0.3	0.03390498	370.0633411 (<0.1)	370.0632902 (2.845)	0.000014
	-0.3	0.11641094	370.0313606 (<0.1)	370.0305423 (2.672)	0.000221

Moreover, the capability of the control chart was considered various values of the smoothing constant ($\lambda_1 = 0.05, 0.10, 0.15$ and 0.30). The control charts are more efficient when λ_1 is decreased as illustrated in Figures 2 and 4.

3.2 Applications results

An operating system (OS) is a group of programs that control computer hardware resources and offer shared

services for software applications. The operating system is a crucial part of the computer's system software. Typically, an operating system is necessary for applications to function. Whether it is a desktop or laptop, a smartphone, or your video game console, every computer requires an operating system. The three most widely used operating systems for personal computers are iOS, Microsoft Windows, and Linux. In this case study, two practical datasets are used, which are the percentages of internet users with Windows 7

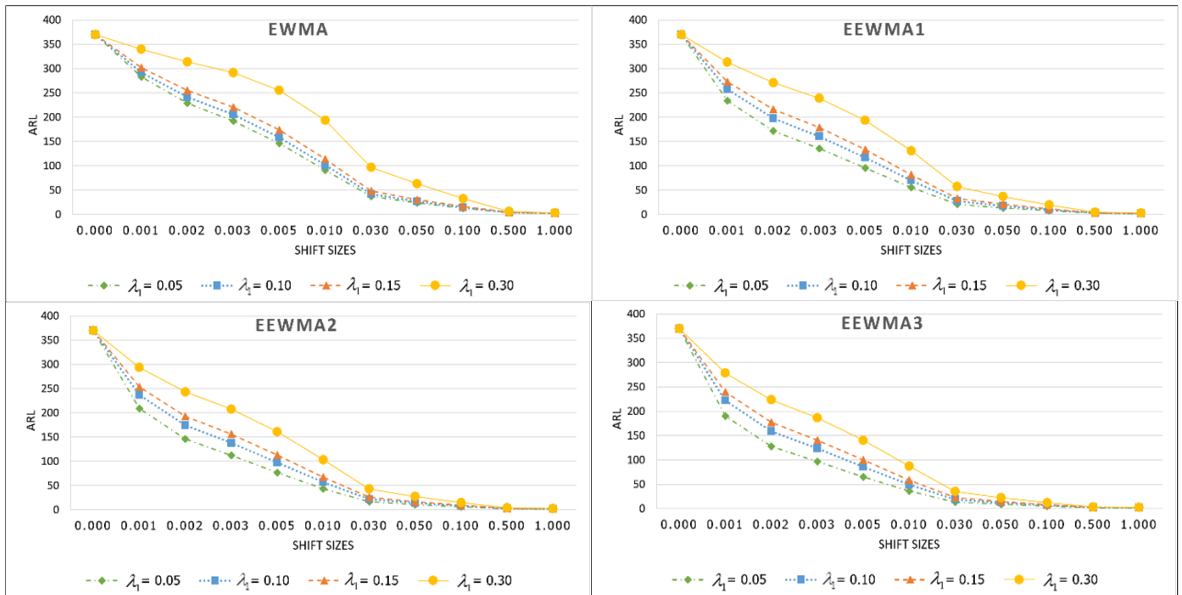


Figure 2: ARL comparing of each control chart based on different λ_1 for the quadratic trend AR(1) model on the EWMA and the EEWMA with various λ_2 control charts.

Table 3: Comparing the ARL for the quadratic trend AR(1) model on the EWMA and EEWMA control chart with different λ at $\phi_1 = 0.2, \eta = 0, \beta = 0.1, \gamma = -0.5$ and $ARL_0 = 370$

λ_1	Chart	b	Shift Sizes											RMI
			0	0.001	0.002	0.003	0.005	0.01	0.03	0.05	0.1	0.5	1	
0.05	EWMA	0.090526	370	283.0	229.1	192.5	146.0	91.3	37.1	23.6	12.7	3.6	2.4	1.1
	EEWMA1	0.0484026	370	234.2	171.4	135.3	95.4	55.2	21.2	13.5	7.4	2.4	1.8	0.4
	EEWMA2	0.0262527	370	209.2	145.9	112.1	76.8	43.3	16.3	10.3	5.8	2.0	1.5	0.2
	EEWMA3	0.0143325	370	190.0	128.0	96.6	65.0	36.0	13.4	8.5	4.8	1.7	1.3	0
0.10	EWMA	0.1900655	370	292.1	241.2	205.4	158.6	101.1	41.8	26.6	14.3	3.8	2.5	0.8
	EEWMA1	0.1362201	370	257.5	197.6	160.4	116.7	69.7	27.3	17.4	9.5	2.9	2.0	0.3
	EEWMA2	0.0987531	370	236.9	174.3	138.0	97.6	56.7	21.8	13.8	7.6	2.5	1.8	0.1
	EEWMA3	0.0721198	370	222.0	158.7	123.6	85.9	49.0	18.6	11.8	6.5	2.2	1.6	0
0.15	EWMA	0.3006137	370	301.9	254.9	220.6	173.9	113.8	48.1	30.7	16.4	4.2	2.6	0.7
	EEWMA1	0.2368993	370	272.8	216.1	179.0	133.4	81.8	32.7	20.8	11.3	3.3	2.2	0.3
	EEWMA2	0.1885898	370	253.6	193.0	155.9	112.8	67.0	26.1	16.6	9.1	2.8	2.0	0.1
	EEWMA3	0.1512147	370	239.5	177.3	140.8	99.9	58.2	22.4	14.2	7.8	2.5	1.8	0
0.30	EWMA	0.732374	370	339.7	313.9	291.6	255.2	193.8	96.6	63.0	32.5	6.2	3.4	0.9
	EEWMA1	0.626235	370	313.0	271.2	239.2	193.5	131.0	57.3	36.7	19.5	4.7	2.8	0.4
	EEWMA2	0.541446	370	293.6	243.3	207.7	160.8	103.0	42.7	27.2	14.6	3.9	2.5	0.1
	EEWMA3	0.472013	370	278.6	223.4	186.5	140.4	87.0	35.1	22.3	12.1	3.4	2.3	0

Notation: EEWMA1, EEWMA2, EEWMA3 denote the EEWMA control chart with λ_2 to be 0.01, 0.02, 0.03, respectively

and iOS operating systems in Thailand. The fitting of forecast time series dataset models was investigated for two datasets using the autocorrelation function (ACF) and partial autocorrelation function (PACF). Both datasets are time series that are stationary. Researchers confirmed that an exponential distribution

follows white noise by the Kolmogorov-Smirnov test (p -value > 0.05).

For the quadratic trend AR(1) model, the dataset is the percentages of internet users with an operating system of Windows 7 collected monthly from April 2010 to March 2015, and this model can be assigned as follows:

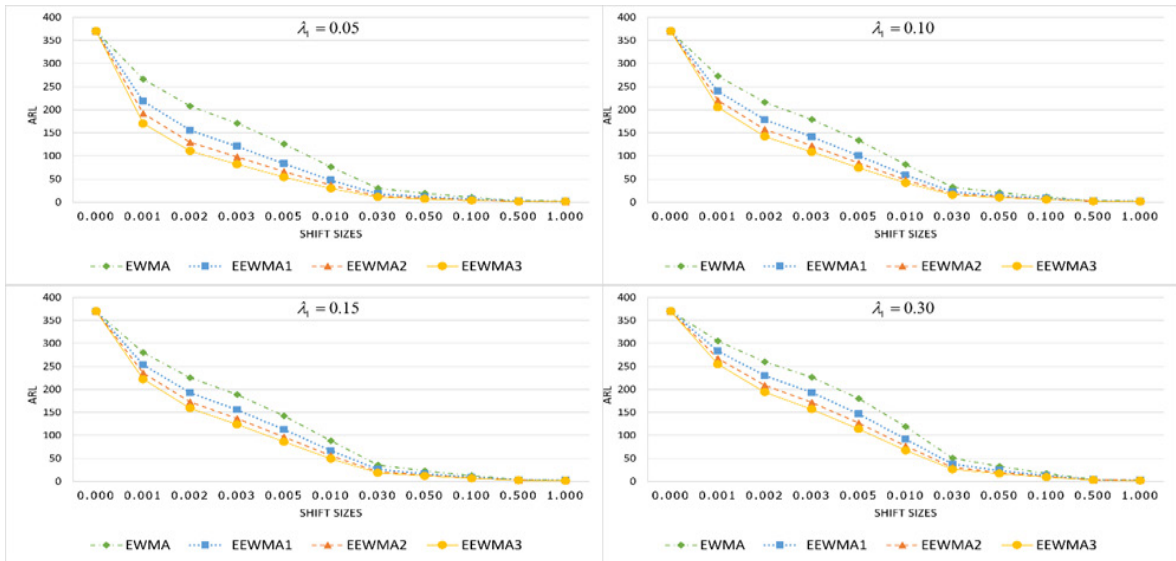


Figure 3: ARL comparing of the EWMA and the EEWMA with different λ_2 control charts for the quadratic trend AR(2) model based on various λ_1 situations.

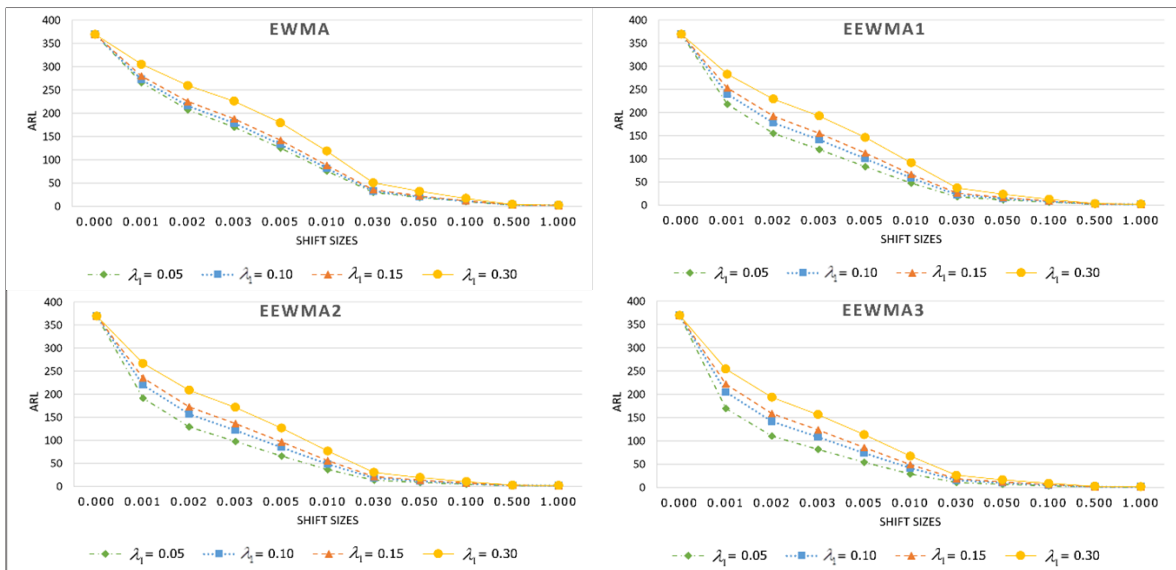


Figure 4: ARL comparing each control chart based on different λ_1 for the quadratic trend AR(2) model on the EWMA and the EEWMA with various λ_2 control charts.

$$X_t = 2.181064t - 0.029043t^2 + 0.775081X_{t-1} + \varepsilon_t$$

where $\varepsilon_t \sim Exp(0.3888)$.

For the quadratic trend AR(2) model, the dataset is the percentages of internet users with an operating system of iOS collected monthly from October 2011 to September

2016, and this model can be assigned as follows:

$$X_t = 4.074542 + 0.685726t - 0.006359t^2 + 0.807431X_{t-1} - 0.296551X_{t-2} + \varepsilon_t$$

where $\varepsilon_t \sim Exp(0.4938)$.

Table 4: The *ARL* comparing for the quadratic trend AR(2) model on the EWMA and the EEWMA control charts with different λ at $\phi_1 = \phi_2 = 0.2, \eta = 0, \beta = 0.1, \gamma = -0.5$ and $ARL_0 = 370$

λ_1	Chart	<i>b</i>	Shift Sizes											RMI
			0	0.001	0.002	0.003	0.005	0.01	0.03	0.05	0.1	0.5	1	
0.05	EWMA	0.07348406	370	261.5	202.3	165.1	120.8	72.6	28.6	18.2	10.0	3.0	2.1	1.1
	EEWMA1	0.03222897	370	216.6	153.3	118.8	82.0	46.6	17.6	11.2	6.2	2.1	1.6	0.4
	EEWMA2	0.01435306	370	190.1	128.1	96.7	65.0	36.0	13.4	8.5	4.8	1.7	1.3	0.2
	EEWMA3	0.006428656	370	168.7	109.4	81.1	53.6	29.2	10.8	6.9	3.9	1.5	1.2	0
0.10	EWMA	0.1527953	370	267.6	209.7	172.5	127.4	77.4	30.7	19.5	10.7	3.2	2.2	0.7
	EEWMA1	0.09925664	370	237.5	175.0	138.7	98.2	57.0	21.9	13.9	7.7	2.5	1.8	0.3
	EEWMA2	0.06530968	370	218.3	155.0	120.3	83.2	47.3	17.9	11.4	6.3	2.1	1.6	0.1
	EEWMA3	0.04329577	370	203.4	140.4	107.3	73.1	41.0	15.4	9.7	5.4	1.9	1.4	0
0.15	EWMA	0.238938	370	274.1	217.8	180.7	135.0	82.9	33.2	21.1	11.5	3.3	2.2	0.5
	EEWMA1	0.1765303	370	249.6	188.5	151.5	108.9	64.3	25.0	15.9	8.7	2.7	1.9	0.3
	EEWMA2	0.131895	370	232.9	170.1	134.0	94.3	54.5	20.9	13.2	7.3	2.4	1.7	0.1
	EEWMA3	0.09928833	370	220.0	156.7	121.8	84.4	48.1	18.2	11.6	6.4	2.1	1.6	0.0
0.30	EWMA	0.553448	370	296.8	247.8	212.8	165.9	107.2	44.8	28.6	15.3	4.0	2.6	0.5
	EEWMA1	0.4609378	370	277.1	221.6	184.7	138.6	85.7	34.5	21.9	11.9	3.4	2.3	0.2
	EEWMA2	0.3879571	370	262.3	203.3	166.1	121.7	73.2	28.8	18.3	10.0	3.0	2.1	0.1
	EEWMA3	0.3290862	370	250.6	189.6	152.5	109.8	64.9	25.2	16.0	8.8	2.7	1.9	0.0

Table 5: The *ARL* comparing for the quadratic trend AR(1) model on the EWMA and the extended EWMA control charts under the observations of percentage of operation system users by Windows 7 at $ARL_0 = 370$

λ_1	Chart	<i>b</i>	Shift Sizes											RMI
			0	0.001	0.002	0.003	0.005	0.01	0.03	0.05	0.1	0.5	1	
0.05	EWMA	0.0315564	370	268.7	211.0	173.7	132.9	79.8	31.8	20.3	11.0	3.3	2.2	2.2
	EEWMA1	0.00651451	370	192.2	130.0	98.3	69.1	37.6	14.0	9.0	5.0	1.8	1.4	0.7
	EEWMA2	0.00138389	370	152.6	96.3	70.5	48.1	25.4	9.4	6.0	3.4	1.4	1.2	0.2
	EEWMA3	0.000295437	370	124.4	75.0	53.8	36.1	18.8	6.9	4.5	2.6	1.2	1.1	0
0.10	EWMA	0.0659004	370	276.1	220.2	183.2	141.7	86.3	34.7	22.2	12.0	3.4	2.3	1.3
	EEWMA1	0.0289555	370	221.6	158.3	123.2	88.9	49.8	18.9	12.1	6.7	2.2	1.6	0.5
	EEWMA2	0.0131174	370	193.1	130.8	99.0	69.6	37.9	14.1	9.0	5.0	1.8	1.4	0.2
	EEWMA3	0.00601396	370	171.0	111.4	82.7	57.1	30.6	11.3	7.2	4.1	1.5	1.2	0
0.15	EWMA	0.1035726	370	284.0	230.5	194.0	152.0	94.1	38.4	24.6	13.2	3.7	2.4	1.1
	EEWMA1	0.0582247	370	237.5	175.0	138.6	101.8	58.2	22.4	14.3	7.9	2.5	1.8	0.4
	EEWMA2	0.0337127	370	212.5	149.2	115.0	82.3	45.7	17.2	11.0	6.1	2.1	1.5	0.1
	EEWMA3	0.019811	370	193.9	131.5	99.6	70.1	38.2	14.3	9.1	5.1	1.8	1.4	0
0.30	EWMA	0.2451441	370	313.1	271.1	239.1	198.1	133.0	58.3	37.6	19.9	4.7	2.9	1.0
	EEWMA1	0.17294	370	271.9	215.0	177.9	136.7	82.5	33.0	21.1	11.4	3.3	2.2	0.4
	EEWMA2	0.1259182	370	247.6	186.2	149.3	111.0	64.4	25.0	15.9	8.7	2.7	1.9	0.1
	EEWMA3	0.093422	370	230.7	167.7	131.9	96.1	54.4	20.8	13.2	7.3	2.3	1.7	0

Based on the quadratic trend AR(1) model in Table 5, the *ARL* evaluating the EWMA against the EEWMA control charts is assessed. And then, the *ARL* of control charts for the quadratic trend AR(2) model is presented in Table 6. The results of both datasets are comparable to those of simulated data, and it is discovered that the EEWMA control charts outperform

the EWMA control chart with small shift detection, so these charts are adjusted λ_2 to be larger, as illustrated in Figures 5 and 7. When the *ARLs* were compared with various control charts based on different λ_1 , the results showed that $\lambda_1 = 0.05$ provided the least *ARL*, as illustrated in Figures 6 and 8, and then demonstrated how the outcomes matched those of the simulation.

Table 6: Comparing ARL for the quadratic trend $AR(2)$ model on the EWMA and EEWMA control charts under the observations of the percentage of operation system users by iOS at $ARL_0 = 370$

λ_1	Chart	b	Shift Sizes											RMI
			0	0.001	0.002	0.003	0.005	0.01	0.03	0.05	0.1	0.5	1	
0.05	EWMA	0.0195667	370	224.2	161.0	125.7	87.5	50.9	19.3	12.2	6.8	2.3	1.7	1.8
	EEWMA1	0.002535406	370	162.2	104.1	76.8	50.5	27.9	10.2	6.5	3.7	1.4	1.2	0.7
	EEWMA2	0.000333965	370	123.9	74.6	53.5	34.3	18.6	6.8	4.4	2.6	1.2	1.1	0.2
	EEWMA3	0.0000440676	370	99.3	57.6	40.6	25.7	13.9	5.1	3.4	2.0	1.1	1.0	0.0
0.10	EWMA	0.03993977	370	226.8	163.7	128.2	89.5	52.2	19.8	12.6	6.9	2.3	1.7	0.9
	EEWMA1	0.01411205	370	189.6	127.7	96.3	64.8	36.5	13.5	8.6	4.8	1.7	1.3	0.4
	EEWMA2	0.005081245	370	162.5	104.3	76.9	50.6	28.0	10.3	6.5	3.7	1.4	1.2	0.2
	EEWMA3	0.001840641	370	141.0	87.3	63.3	41.0	22.4	8.2	5.3	3.0	1.3	1.1	0.0
0.15	EWMA	0.0611885	370	229.5	166.5	130.8	91.6	53.6	20.4	12.9	7.1	2.3	1.7	0.7
	EEWMA1	0.03013294	370	201.5	138.6	105.8	71.9	40.9	15.2	9.7	5.4	1.9	1.4	0.3
	EEWMA2	0.01510878	370	180.4	119.4	89.4	59.6	33.4	12.3	7.8	4.4	1.6	1.3	0.1
	EEWMA3	0.0076376	370	162.7	104.5	77.1	50.7	28.0	10.3	6.5	3.7	1.4	1.2	0
0.30	EWMA	0.1310330	370	238.1	175.7	139.3	98.7	58.3	22.3	14.1	7.7	2.5	1.8	0.4
	EEWMA1	0.0895099	370	219.7	156.4	121.5	84.2	48.7	18.3	11.6	6.4	2.1	1.6	0.2
	EEWMA2	0.0620826	370	205.1	142.1	108.8	74.2	42.4	15.8	10.0	5.5	1.9	1.4	0.1
	EEWMA3	0.0434716	370	192.8	130.5	98.8	66.6	37.6	13.9	8.8	4.9	1.7	1.4	0

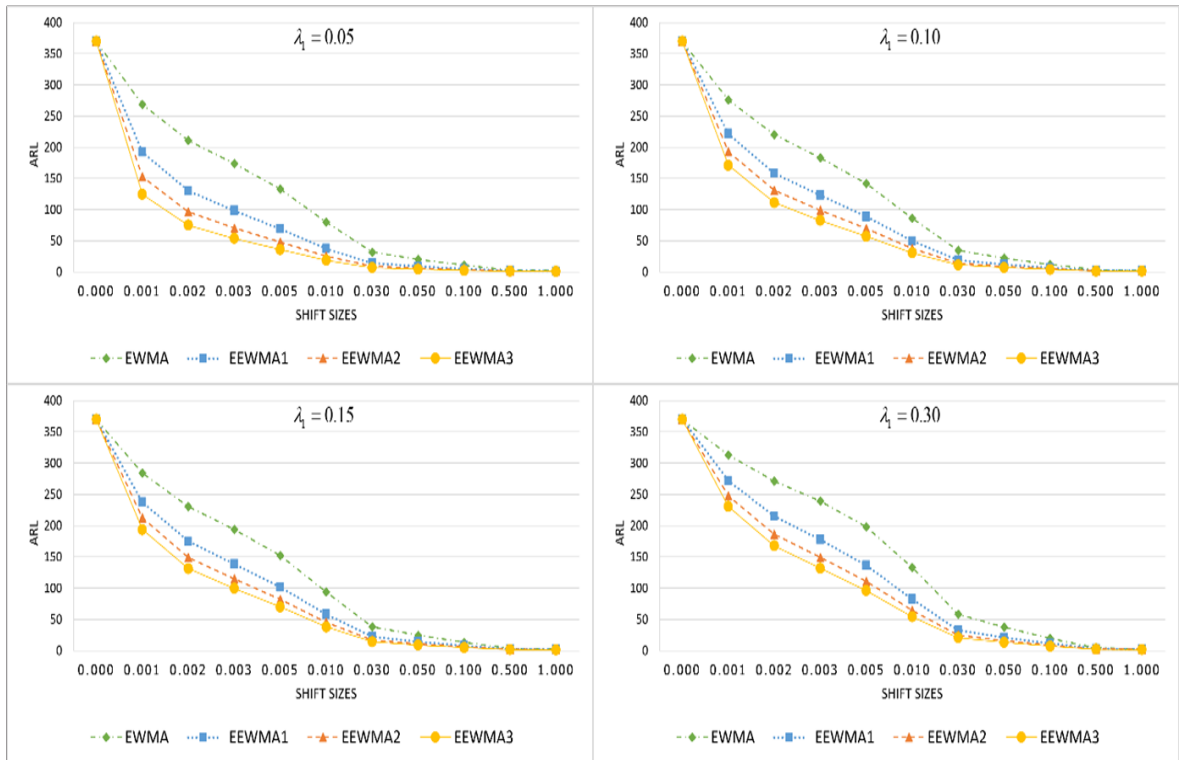


Figure 5: ARL comparing of the EWMA and the EEWMA with different λ_2 control charts for the quadratic trend $AR(1)$ model based on various λ_1 situations for the percentages of internet users with Windows 7 in Thailand.

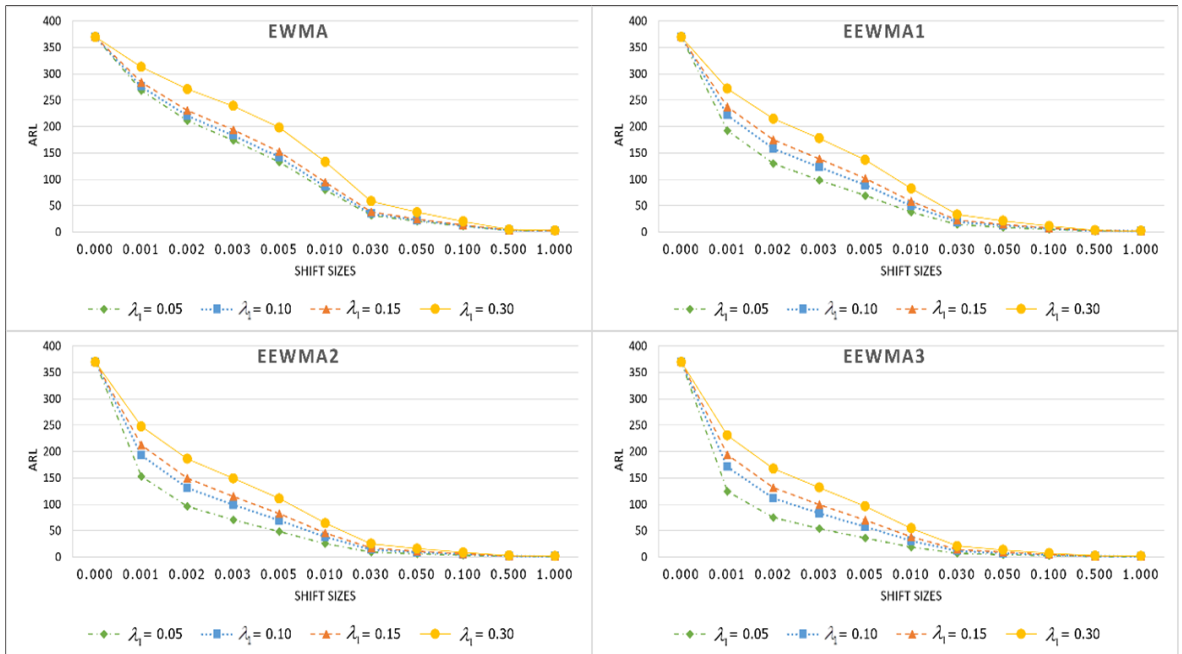


Figure 6: ARL comparing each control chart based on different λ_1 for the quadratic trend AR(1) model on the EWMA and the EEWMA with various λ_2 control charts for the percentages of internet users with Windows 7 in Thailand.

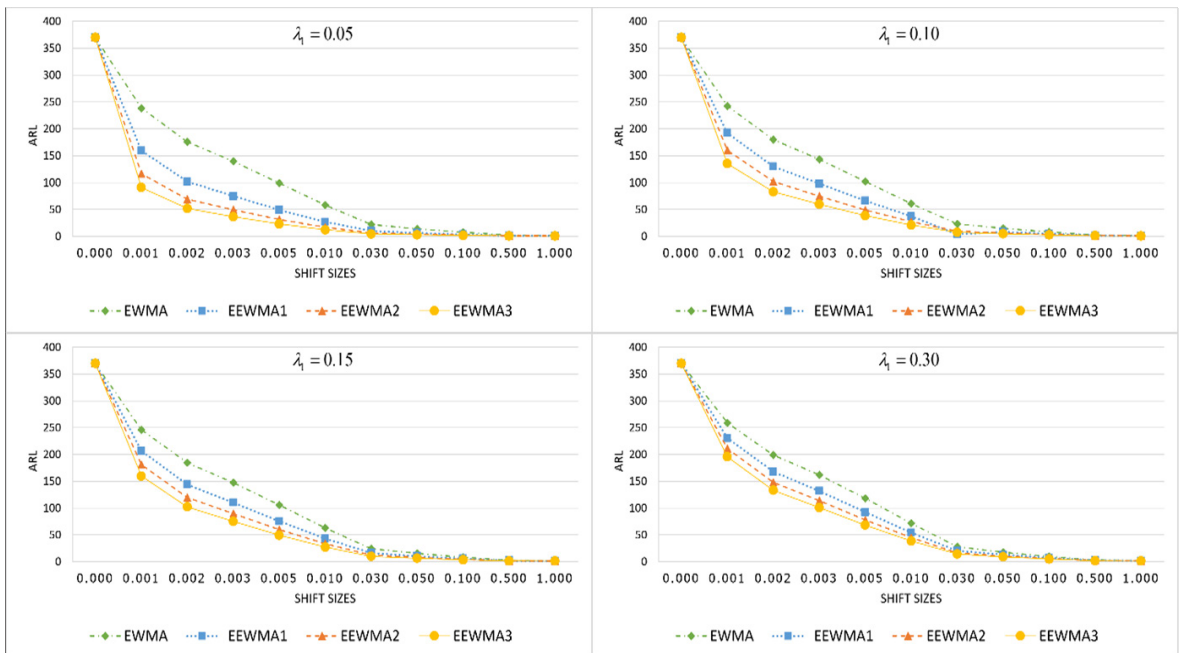


Figure 7: ARL comparing of the EWMA and the EEWMA with different λ_2 control charts for the quadratic trend AR(2) model based on various λ_1 situations for the percentages of internet users with iOS in Thailand.

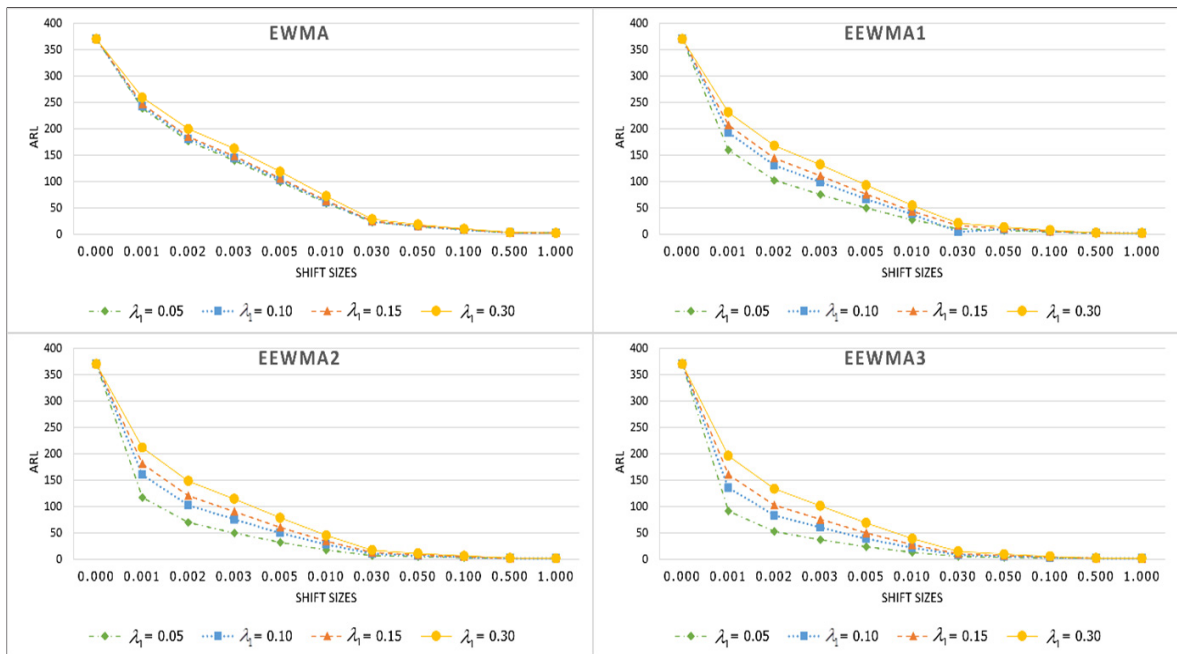


Figure 8: *ARL* comparing of each control chart based on different λ_1 for the quadratic trend AR(2) model on the EWMA and the EEWMA with various λ_2 control charts for the percentages of internet users with iOS in Thailand.

4 Discussions and Conclusions

The *ARL* was utilized in the research to evaluate the effectiveness of control charts. The explicit formulas provide a suitable NIE method for building the *ARL* substitute. The quadratic trend AR(1) and quadratic trend AR(2) represent the analytical results for the model. The results are shown with the NIE approximations, with an absolute relative change of less than 0.00023%. When using the explicit formulas, the *ARL* calculation took nearly no time at all in terms of computational time but took about 3 s when utilizing the NIE methods. The *ARL* performance comparison using explicit formulas on the EEWMA control charts with different λ outperformed the EWMA control chart running the quadratic trend AR(1) or AR(2) models when δ is small. Correspondingly, the relative mean index (*RMI*) is used to examine the *ARL*'s comparative performance under various λ_2 conditions. The EEWMA control chart has given a higher capability for detecting shifts if λ_2 has been higher. When the comparative performance of the *ARL* under various λ_1 conditions is examined. The simulation studies and the performance illustration with real-world datasets that are using data

to represent the percentages of Windows 7 and iOS in Thailand provided similar results. Hence, an exponential smoothing parameter of 0.05 was proposed to be used, and that is used based on the EEWMA control chart when the data are of the exponential white noise distribution.

Acknowledgments

The authors would like to express our gratitude to the editor and referees for their valuable comments and suggestions which greatly improve this manuscript. The research was funded by King Mongkut's University of Technology North Bangkok Contract no. KMUTNB-65-BASIC-15.

Author Contributions

Kotchaporn Karoon: conceptualization, data analysis, methodology, data curation, writing an original draft, and writing—reviewing and editing; Yupaporn Areepong: conceptualization, funding acquisition, investigation; Saowanit Sukparungsee: investigation. All authors have read and agreed to the published version of the manuscript.

Conflicts of Interest

The authors declare no conflict of interest.

References

- [1] S. Ozilgen, "Statistical quality control charts: New tools for studying the body mass index of populations from the young to the elderly," *Nutrition, Health & Aging*, vol. 15, no. 5, pp. 333–339, 2011.
- [2] M. Kovarik, L. Sarga, and P. Klimek, "Usage of control charts for time series analysis in financial management," *Business Economics and Management*, vol. 16, no. 1, pp. 138–158, 2015.
- [3] W. A. Shewhart, *Economic Control of Quality of Manufactured Product*. New York: Van Nostrand, 1931.
- [4] W. S. Roberts, "Control chart tests based on geometric moving average," *Technometrics*, vol. 1, no. 3, pp. 239–250, 1959.
- [5] E. S. Page, "Continuous inspection schemes," *Biometrika*, vol. 41, no. 1–2, pp. 100–115, 1954.
- [6] A. K. Patel and J. Divecha, "Modified exponentially weighted moving average (EWMA) control chart for an analytical process data," *Chemical Engineering and Materials Science*, vol. 2, pp. 12–20, 2011.
- [7] N. Khan, M. Alsam, and C.H. Jun, "Design of a control chart using a modified EWMA statistics," *Quality and Reliability Engineering International*, vol. 33, no. 5, pp. 1095–1104, 2017.
- [8] M. Neveed, M. Azam, N. Khan, and M. Aslam, "Design a control chart using extended EWMA statistic," *Technologies*, vol. 6, no. 4, pp. 108–122, 2018.
- [9] C. M. Mastrangelo and D. C. Montgomery, "SPC with correlated observations for the chemical and process industries," *Quality Reliability Engineering International*, vol. 11, no. 2, pp. 79–89, 1995.
- [10] C. Chanant, Y. Areepong, and S. Sukparungsee, "A Markov chain approach for average run length of EWMA and CUSUM control chart based on ZINB model," *International Journal of Applied Mathematics and Statistics*, vol. 53, no. 1, pp. 126–137, 2015.
- [11] S. Sukparungsee, "Combining martingale and integral equation approaches for finding optimal parameters of EWMA," *Applied Mathematical Sciences*, vol. 6, pp. 4471–4482, 2012.
- [12] K. Karoon, Y. Areepong, and S. Sukparungsee, "Numerical integral equation methods of average run length on extended EWMA control chart for autoregressive process," in *International Conference on Applied and Engineering Mathematics*, 2021, pp. 51–56.
- [13] W. Suriyakit, Y. Areepong, S. Sukparungsee, and G. Mititelu, "Analytical method of average run length for trend exponential AR(1) processes in EWMA procedure," *IAENG International Journal of Applied Mathematics*, vol. 42, no. 4, pp. 250–253, 2012.
- [14] K. Petcharat, Y. Areeporn, and S. Sukparungsee, "Exact solution of average run length of EWMA chart for MA(q) processes," *Far East Journal of Mathematical Sciences*, vol. 2, no. 2, pp. 291–300, 2013.
- [15] P. Busababodin, "An analytical expression to CUSUM chart for seasonal AR(p) model," *Far East Journal of Mathematical Sciences*, vol. 88, no. 1, pp. 89–105, 2014.
- [16] P. Paichit, "Exact expression for average run length of control chart of ARX(p) procedure," *KKU Science Journal*, vol. 45, no. 4, pp. 948–958, 2017.
- [17] S. Phanyaem, "Average run length of cumulative sum control charts for SARMA(1,1)L models," *Thailand Statistician*, vol. 15, pp. 184–195, 2017.
- [18] S. Sukparungsee and Y. Areepong, "An explicit analytical solution of the average run length of an exponentially weighted moving average control chart using an autoregressive model," *Chiang Mai Journal of Science*, vol. 44, no. 3, pp. 1172–1179, 2017.
- [19] Y. Areepong, "Explicit formulas of average run length for a moving average control chart monitoring the number of defective products," *IJAM*, vol. 80, pp. 331–343, 2019.
- [20] S. M. Anwar, M. Aslam, S. Ahmad, and M. Riaz, "A modified-mxEWMA location chart for the improved process monitoring using auxiliary information and its application in wood industry," *Quality Technology and Quantitative Management*, vol. 17, no. 5, pp. 561–579, 2020.
- [21] R. Sunthornwat and Y. Areepong, "Average run length on CUSUM control chart for seasonal and

- non-seasonal moving average processes with exogenous variable,” *Symmetry*, vol. 12, no. 1, pp. 173–187, 2020.
- [22] A. Saghir, M. Aslam, A. Faraz, and L. Ahmad, “Monitoring process variation using modified EWMA,” *Quality and Reliability Engineering International*, vol. 36, no. 1, pp. 328–339, 2020.
- [23] P. Phanthuna, Y. Areepong, and S. Sukparungsee, “Exact run length evaluation on a two-sided modified exponentially weighted moving average chart for monitoring process mean,” *Computer Modeling in Engineering and Sciences*, vol. 127, no. 1, pp. 23–41, 2021.
- [24] P. Phanthuna, Y. Areepong, and S. Sukparungsee, “Detection capability of the modified EWMA chart for the trend stationary AR(1) model,” *Thailand Statistician*, vol. 19, no. 1, pp. 70–81, 2021.
- [25] K. Karoon, Y. Areepong, and S. Sukparungsee, “Exact run length evaluation on extended EWMA control chart for autoregressive process,” *Intelligent Automation and Soft Computing*, vol. 33, no. 2, pp. 743–758, 2022.
- [26] C. W. Champ and S. E. Rigdon, “A comparison of the Markov chain and the integral equation approaches for evaluating the run length distribution of quality control charts,” *Communications in Statistics-Simulation and Computation*, vol. 20, no. 1, pp. 191–203, 1991.
- [27] Q. T. Nguyen, K. P. Tran, P. Castagliola, G. Celano, and S. Lardiane, “One-sided synthetic control charts for monitoring the multivariate coefficient of variation,” *Journal of Statistical Computation and Simulation*, vol. 89, no. 1, pp. 1841–1862, 2019.
- [28] A. Tang, P. Castagliola, J. Sun, and X. Hu, “Optimal design of the adaptive EWMA chart for the mean based on median run length and expected median run length,” *Quality Technology and Quantitative Management*, vol. 16, no. 4, pp. 439–458, 2018.